Research Square

Preprints are preliminary reports that have not undergone peer review.
They should not be considered conclusive, used to inform clinical practice,
or referenced by the media as validated information.

The Mimetic Peptide Ac2-26 of Annexin A1 Attenuates Inflammation and Apoptosis in Sepsis-Induced Acute Kidney Injury

Yanlei Zheng
The Intensive Care Unite, Hubei Cancer Hospital, Tongji Medical College, Huazhong University of Science and Technology

Ronghua Hu
The Intensive Care Unite, Hubei Cancer Hospital, Tongji Medical College, Huazhong University of Science and Technology

Li Zhang (moli78411@yahoo.com)
The Intensive Care Unite, Hubei Cancer Hospital, Tongji Medical College, Huazhong University of Science and Technology

Research

Keywords: Sepsis, Acute kidney injury, Inflammation, Apoptosis

Posted Date: December 29th, 2020

DOI: https://doi.org/10.21203/rs.3.rs-135005/v1

License: This work is licensed under a Creative Commons Attribution 4.0 International License.
Read Full License

The mimetic peptide Ac2-26 of annexin A1 attenuates inflammation and apoptosis in sepsis-induced acute kidney injury

Yanlei Zheng[1], Ronghua Hu[1], Li Zhang[1#]

[1]The Intensive Care Unite, Hubei Cancer Hospital, Tongji Medical College, Huazhong University of Science and Technology, Wuhan, 430079, China.

[#]Correspondence: Li Zhang, E-mail:moli78411@yahoo.com

Abstract:

Background: Inflammation and apoptosis contribute to the development of sepsis-induced acute kidney injury. Annexin A1 (ANXA1) is the calcium-dependent phospholipid-binding protein known to play an important role in a variety of cellular functions, including inflammation, apoptosis, migration and proliferation. However, the effect of ANXA1 on sepsis-induced acute injury has not been reported. Herein, we investigated the role and underlying mechanism of the mimetic peptide Ac2-26 of annexin A1 in sepsis-induce acute kidney injury in vivo and in vitro.

Methods: In vivo, a mouse model was established by cecal ligation and puncture (CLP), and the Ac2-26 peptide of ANXA1 (1 mg/kg) was intraperitoneally administered 2 hours before CLP. In vitro, A model of HK-2 cells was established by treatment with 10 μg/ml lipopolysaccharide (LPS), and the Ac2-26 peptide of ANXA1 (0.5 μmol/L) was administered 2 hours before LPS. The kidney function of mice detected by Elisa. The kidney tissue was examined by HE and TEM. The inflammatory cytokines and apoptotic molecules were measured by PCR, Elisa, Western blotting and Immunohistochemistry. The apoptosis was detected by TUNEL and flow cytometry.

Results: The studies demonstrated that ANXA1 markedly improved kidney function and kidney tissue injury and enhanced 7-day survival in CLP-induced septic mice, which was accompanied by a significant decrease the inflammatory molecules. ANXA1 obviously downregulated the apoptosis-associated proteins and inhibited apoptosis in kidney tissue in vivo. In vitro studies showed that ANXA1 increased the viability of HK-2 cells, reduced the levels of the inflammatory molecules, downregulated the apoptosis-associated proteins Bax, upregulated the antiapoptotic protein Bcl-2 and inhibited the apoptosis of HK-2 cells.

Conclusions: The mimetic peptide Ac2-26 of annexin A1 protects against sepsis-induced inflammation, apoptosis, and kidney dysfunction via regulating the LXA4/PI3K/IKK-β/NF-κB signaling pathway.

Key words: Sepsis, Acute kidney injury, Inflammation, Apoptosis

Background

Currently, sepsis remains one of the leading clinical conditions in intensive care units (ICU) and causes a huge economic burden worldwide [1]. The kidney is one of the most vulnerable organs and is associated with severe complications in sepsis [2], which is an important cause of Acute Kidney Injury (AKI) in ICU patients [3-4]. Septic AKI is associated with poor prognosis and high mortality in critically ill patients [5-6]. Related studies have reported that the mortality rate of patients with

septic AKI is approximately twice as high as that of patients with sepsis without AKI [7]. With advances in clinical treatment, such as fluid resuscitation and kidney replacement therapy, these treatments may improve survival, but the mortality rate of patients with AKI is still as high as 30% [8]. There is still no specific treatment for septic AKI and its mechanisms are not fully understood.

Several studies have suggested that the pathogenesis of septic AKI is due to intrarenal hemodynamic abnormalities, the inflammatory response, immune cell infiltration and renal tubular cell apoptosis [6, 9-11]. Further research has found that the inflammatory response and apoptosis in renal tissue are closely related to the occurrence of septic AKI [12-13]. When the host has a severe bacterial infection, a large increase in lipopolysaccharide (LPS) in the serum leads to a significant increase in proinflammatory factors, which eventually induce tissue damage and organ failure and is also known as sepsis [14]. LPS is an endotoxin that is produced by the outer membrane of gram-negative bacteria. LPS has been widely used in sepsis and septic kidney injury research [15].

Annexin A1 (ANXA1) is a member of the calcium-dependent phospholipid-binding protein family of Annexins and is a 37 kDa protein composed of 346 amino acids [16-17]. ANXA1 exhibits a variety of biological activities, such as regulation of the inflammation, cell signal transduction, cell differentiation and apoptosis [18-19]. Previous reports suggest that ANXA1 activates the formyl peptide receptor 2-lipoxin receptor (FPR2/ALX or lipoxin A4 receptor, LXA4) to exert biological functions through the N-terminal region of the Ac2-26 peptide [17, 20-22]. In addition, related studies have found that LXA4 suppresses the inflammatory response and tissue apoptosis during sepsis in mice [22-24]. Therefore, ANXA1 may be beneficial in sepsis-associated AKI by negatively regulating the inflammatory response and apoptosis.

In this study, we hypothesized that the mimetic peptide Ac2-26 of ANXA1 has a protective effect in septic AKI. To verify this hypothesis, we established mouse and cell sepsis models by cecal ligation and puncture (CLP) surgery and LPS stimulation, respectively, to investigate the effects and underlying molecular mechanisms of the Ac2-26 mimetic peptide of ANXA1 in sepsis-induced AKI.

Materials and Methods

The ANXA1 mimetic peptide Ac2-26 (acetyl-AMVSEFLKQAWFIEEQEYVQTVK) was purchased from Hangzhou Angtai Biotechnology Co. Ltd. (China). The Cre and BUN ELISA kits were obtained from Nanjing Jiancheng Bioengineering Institute (China). The LXA4 ELISA kit was purchased from Cloud-Clone Corp. (Wuhan, China). MyD88, P-IKKβ, IKKβ, P-PI3K, PI3K, NF-κB, cleaved caspase3, Caspase8 and FADD primary antibodies were obtained from Abcam (USA). The Bcl-2 and Bax primary antibodies were purchased from Cell Signaling Technology, Inc. (Danvers, MA, USA). The TUNEL kit was purchased from Roche In Situ Cell Death Detection Kit (USA). The CCK-8 kit was obtained from Dojindo Molecular Technologies (Gaithersburg, MD, USA). The Annexin V-FITC flow cytometry apoptosis kit was purchased from Tianjin Sungene Biotech Co., Ltd. (China).

Animals, Groupings and Modeling

Male wild-type C57BL/6 mice (6-8 weeks old, weighing 20-30 g) were obtained from the Center of Experimental Animals of Wuhan University in China. The mice were maintained in a standard environment (12-h light/dark cycle, temperature of 25°C, humidity of 50%) with free access to food and water for 1 week before the experiments. Animal experiments were performed in accordance with Chinese legislation on the use and care of laboratory animals and were approved by the Animal Care and Use Committee of Hubei Cancer Hospital, China. The mice experiments were performed in the animal laboratory of Hubei Provincial Cancer Hospital.

The 120 mice were randomly divided into three groups: the Control group (Con), Sepsis group (Sep) and Ac2-26+Sepsis group (Ac+Sep). Mice were anesthetized with 1% sodium pentobarbital (50 mg/kg). The experimental model of sepsis was established by cecal ligation and puncture (CLP) surgery [25]. The mice in the Ac2-26+sepsis group were intraperitoneally injected with Ac2-26 (1 mg/kg) 2 h before CLP. Except for the mice that were used for the survival test, the rest of the mice were subjected to related experiments 24 h after CLP. Mice were anesthetized by sodium pentobarbital and then sacrificed with cervical dislocation before the procurement of their tissue specimens. The experiment was repeated six times.

Detection of Cre, BUN and LXA4 Levels by ELISA

Serum was collected from each mouse. The levels of serum creatinine (Cre), blood urea nitrogen (BUN) and LXA4 were detected by ELISA kits according to the manufacturer's instructions.

Reverse Transcription-Quantitative Polymerase Chain Reaction (RT-qPCR)

The mRNA expression of TNF-α, IL-1β and IL-6 in kidney tissue was measured by RT-qPCR. First, total RNA was extracted by TRIzol reagent (Invitrogen Life Technologies, CA, USA). Then, cDNA was synthesized from the RNA with PrimeScriptTM RT Master Mix (Takara, Japan) for quantitative RT-PCR. The mRNA level was determined via a Light Cycler 480 (Roche, Basel, Switzerland) and was normalized to GAPDH (glyceraldehyde-3-phosphate dehydrogenase). The sequences of the sample primers are shown in Table 1.

Table 1 Primer sequences for quantitative RT-PCR

Genes	Forward primer sequence (5′→3′)	Reverse primer sequence (5′→3′)
TNF-α	CACCACGCTCTTCTGTCTACTG	GCTACGGGCTTGTCACTCG
IL-1β	AGTTGACGGACCCCAAAAG	AGCTGGATGCTCTCATCAGG
IL-6	GACAAAGCCAGAGTCATTCAGAG	GTCTTGGTCCTTAGCCACTCC
GAPDH	GCCAAGGTCATCCATGACAAC	GTGGATGCAGGGATGATGTTC

Western Blot Analysis

The protein levels of MyD88, P-IKKβ, IKKβ, P-PI3K, PI3K, NF-κB, cleaved caspase3, Caspase8 and FADD in kidney tissue were measured by western blotting. First, the proteins were extracted with RIPA lysis buffer from kidney tissue, and the concentration was determined via a bicinchoninic acid (BCA) assay. Each sample was electrophoresed on an SDS-polyacrylamide gel and transferred to PVDF membranes. The PVDF membranes were blocked with PBS containing 5% skim milk and

incubated with primary antibodies (anti-MyD88, 1:1000; anti-P-IKKβ, 1:1000; anti-IKKβ, 1:1000; anti-P-PI3K, 1:1000; anti-PI3K, 1:1000; anti-NF-κB, 1:1000; anti-cleaved caspase3, 1:800; anti-Caspase8, 1:800; and anti-FADD, 1:800) in a shaker at 4°C overnight. Next, the membranes were washed with TBST and then incubated with secondary antibodies (LI-COR, Lincoln, NE, USA; 1:5000 dilution) for 1 h at room temperature. Finally, PVDF membranes were visualized by a LI-COR Odyssey Infrared Imaging System (LI-COR Biosciences Inc., USA).

Hematoxylin and Eosin Staining of Kidney Tissue

The kidney tissue was collected and fixed with a 10% formaldehyde solution for 24 h at room temperature, embedded in paraffin and cut into 3-mm slices. Then, the sections were stained with hematoxylin and eosin (HE) and assessed for morphological changes and damage under a light microscope.

Transmission Electron Microscopy Analysis of kidney tissue

The kidney tissue was harvested and fixed with a 2.5% formaldehyde in PBS solution. Next, the tissue was postfixed with OsO4 for 1 h at room temperature, washed with PBS, dehydrated in ethanol, embedded in epoxy resin and cut into ultrathin sections. The tissue sections were detected via an H-7100 transmission electron microscope (TEM) (Hitachi Co., Japan) operating at 75 kV.

Terminal dUTP Nick End-Labeling (TUNEL) Assay

The kidney tissue was collected and fixed with 10% formaldehyde, embedded in paraffin and sliced into sections. The tissue sections were stained with a TUNEL kit according to the manufacturer's instructions. The sections were stained with 4′,6-diamidino-2-phenylindole (DAPI) for 15 min, washed with PBS and observed under a fluorescence microscope. The apoptotic index (AI) = positive cells/total cells ×100.

HK-2 cells, Treatments and Groupings

HK-2 cells were cultured in DMEM (Gibco, Thermo Fisher Scientific, Waltham, MA, USA) containing 10% fetal bovine serum (FBS, Gibco, Thermo Fisher Scientific, Waltham, MA, USA). HK-2 cells were randomly assigned into three groups: Control group (Con), in which the cells were only given DMEM ; LPS group (LPS), in which the cells were stimulated with 10 μg/mL LPS in DMEM; and Ac2-26+LPS group (Ac+LPS), in which the cells were treated with Ac2-26 (0.5 μmol/L) for 2 h before 10 μg/mL LPS was administered. The cells were stimulated with LPS for 24 h before the experiments. The experiments were repeated six times.

HK-2 cells Viability Assay

The viability of HK-2 cells was determined by a cell counting kit 8 (CCK-8) assay. First, HK-2 cells were cultured in 96-well plates for standard times. Next, CCK-8 solution was added to the cells and incubated in the dark at room temperature for 2 h. The optical density (OD) was read at 450 nm with a microplate reader (Bio-Rad, Hercules, CA, USA). The viability of NRK-52E cells was calculated as (experimental group/control group) × 100.

Detection of TNF-α, IL-1β and IL-6 Levels by ELISA

The supernatant from each group of cells was harvested. The expression of TNF-α, IL-1β and IL-6 in HK-2 cells was detected with ELISA kits according to the

manufacturer's instructions.

Western Blot Analysis

The protein levels of Bcl-2 and Bax were determined by western blotting. First, the proteins from HK-2 cells in each group were extracted with RIPA lysis buffer, and the concentration was determined via a bicinchoninic acid (BCA) assay. The samples were electrophoresed on SDS-polyacrylamide gels and transferred to PVDF membranes. The PVDF membranes were blocked with PBS containing 5% skim milk and incubated with primary antibodies (anti-Bcl-2, 1:800; anti-Bax, 1:1000) in a shaker at 4°C overnight. Next, the membranes were washed with TBST and then incubated with secondary antibodies (LI-COR, Lincoln, NE, USA. 1:5000 dilution) for 1 h at room temperature. Finally, the PVDF membranes were visualized by a LI-COR Odyssey Infrared Imaging System (LI-COR Biosciences Inc., USA).

Immunohistochemistry

The HK-2 cells grew and fused by 80 % on coverslip. The cells were perforated with 1% Triton X-100 in PBS for 5 min and then blocked with 3% FBS for 1 h at room temperature. Subsequently, cells were incubated with the primary antibodies Bcl-2 (1:100) and Bax (1:320). Next, the coverslips were placed in a shaker at 4℃ overnight. The samples were washed by TBST and then incubated the secondary antibodies. Finally, cells were added with 3, 3-diaminobenzidine (DAB) solution. The expression of Bcl-2 and Bax cells was stained brownish as immune-positive cells. The immune-positive cells= positive cells/the total cells ×100.

Flow Cytometry Analysis of HK-2 cell Apoptosis

The apoptosis rate of HK-2 cells was determined by an Annexin V-FITC flow cytometry apoptosis kit. Briefly, 200 μL binding buffer containing 10 μL Annexin V and 5 μL PI was added to the samples for 1 h in the dark. The stained cells were analyzed using a FACSCalibur™ flow cytometer (BD Biosciences, San Jose, CA, USA) and Cell-Quest software.

Statistical Analysis

SPSS version 20.0 statistical software (SPSS, Inc., USA) was used for statistical analysis. All data are repressed as means ± Standard Deviation (SD). Student's t-test was used to compare the differences between two groups. One-way analysis of variance (ANOVA), followed by Bonferroni's post hoc analysis, was performed for comparisons of the differences among more than two groups. P values < 0.05 were considered statistically significant.

Results

Ac2-26 improved the survival and kidney function of mice with sepsis

To explore the effect of Ac2-26 on sepsis-associated AKI, an experimental mouse model of sepsis was induced by CLP. First, the Cre and BUN levels were significantly higher in the sepsis group than in the control group mice (Figure 1A-B). Moreover, the 7-day survival rate of sepsis group mice was decreased compared with that of the control group (Figure 1C). In contrast, treatment with mimetic peptide Ac2-26 of ANXA1 significantly enhanced the survival rate and kidney function in the Ac2-26+sepsis group compared with those in the sepsis group (Figure 1A-C). These results suggest that Ac2-26 alleviates septic AKI and improves the survival of sepsis.

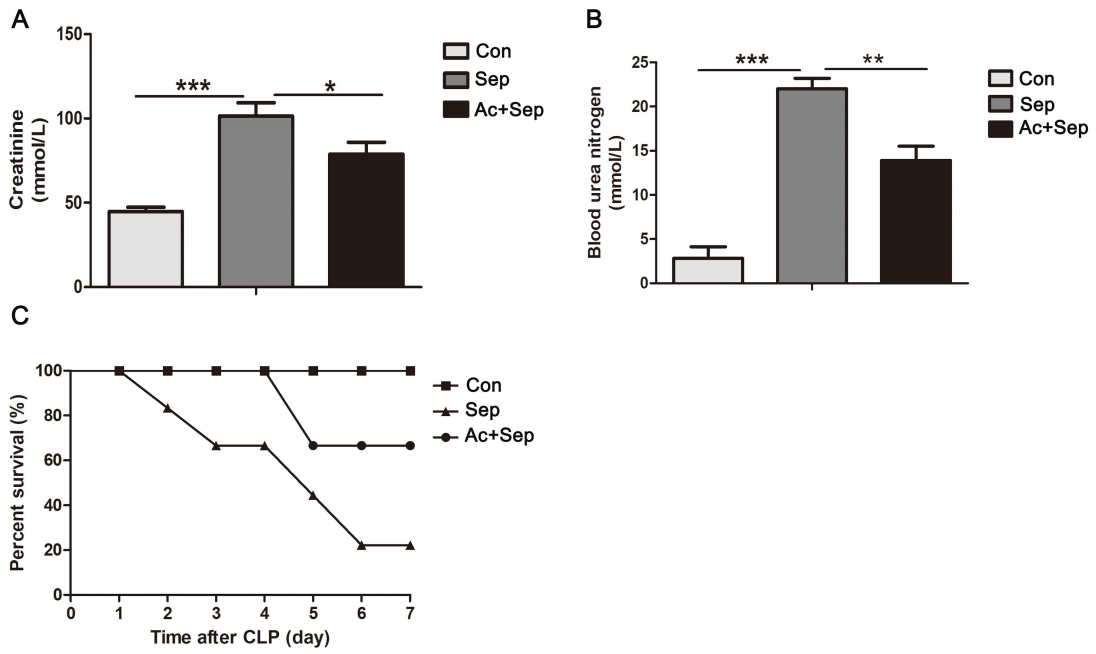

Figure 1. Ac2-26 improved the survival and kidney function of mice with sepsis. (A and B) At 24 h after CLP operation, the levels of Cre and BUN in the kidney tissue were detected by Elisa. (C) the 7 day-survival rate of mice (n= 6 per group). Note: the data are shown as mean ± SD (n = 6 per group, **P* < 0.05, ***P*< 0.01, ****P*<0.001).

Ac2-26 increased the production of LXA4 in the kidney tissue of mice with sepsis

The effects of Ac2-26 on the sepsis-induced level of LXA4 in kidney tissue were measured by ELISA. The data showed that the levels of LXA4 were significantly decreased in the kidneys of the sepsis group compared with those of the control group (Figure 2). However, treatment with mimetic peptide Ac2-26 of ANXA1 increased the level of LXA4 in the Ac2-26+sepsis group compared with that of the sepsis group (Figure 2).

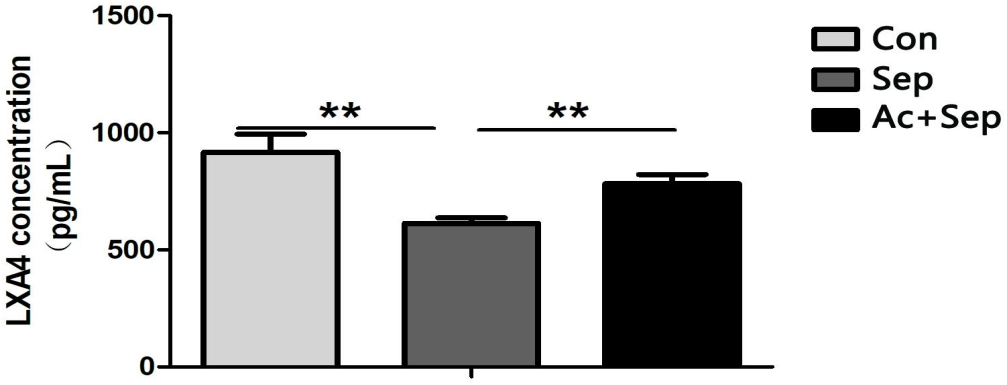

Figure 2. Ac2-26 increased the production of LXA4 in the kidney tissue of mice with sepsis. (A) At 24 h after CLP operation, the LXA4 levels were detected by Elisa. Note: the data are shown as mean ± SD (n = 6 per group, ***P*< 0.01).

Ac2-26 decreased the production of inflammatory-related cytokines in the kidney tissue of mice with sepsis

The effects of Ac2-26 on the production and release of inflammatory-related cytokines induced by sepsis in kidney tissue were measured by RT-PCR and western

blotting. MyD88, P-IKKβ, IKKβ, P-PI3K, PI3K, NF-κB, TNF-α, IL-1β and IL-6 are important inflammatory-related cytokines. The protein expression levels of MyD88, P-IKKβ, P-PI3K, and NF-κB in the kidney tissue of mice in the sepsis group were significantly upregulated compared with those in the control group (Figure 3A). Interestingly, treatment with mimetic peptide Ac2-26 of ANXA1 markedly downregulated the levels of MyD88, P-IKKβ, P-PI3K, and NF-κB in the Ac2-26+sepsis group compared to those in the sepsis group (Figure 3A). In addition, TNF-α, IL-1β and IL-6 were significantly higher in the sepsis group than in the control group (Figure 3B). Interestingly, treatment with mimetic peptide Ac2-26 of ANXA1 significantly reduced these inflammatory cytokines in the Ac2-26+sepsis group compared with those in the sepsis group (Figure 3B). These results suggest that Ac2-26 suppresses the inflammatory response in the kidneys of septic mice.

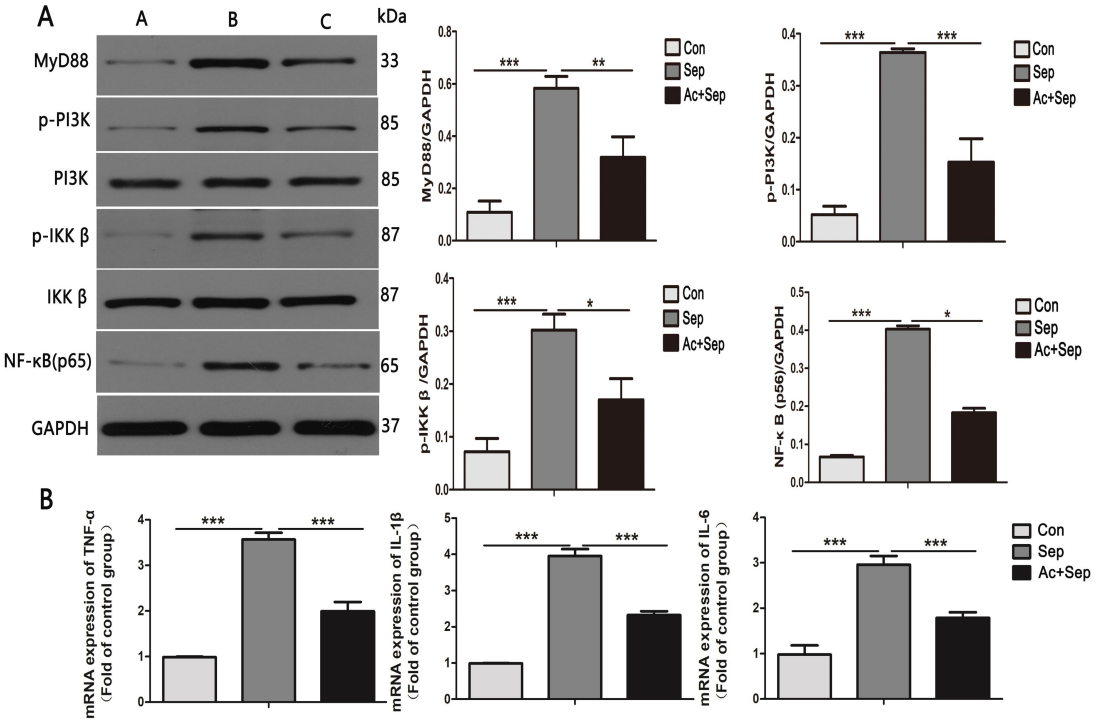

Figure 3. Ac2-26 decreased the production of inflammatory-related cytokines in the kidney tissue of mice with sepsis. (A) At 24 h after CLP operation, the inflammatory cytokines levels were detected by Western blotting, A: Con; B:Sep; C:Ac+Sep; (B) the inflammatory cytokines levels were detected by RT-PCR. Note: the data are shown as mean ± SD (n = 6 per group, **P*<0.05, ***P*< 0.01, ****P*<0.001).

Ac2-26 alleviated pathological damage to the kidney tissue of mice with sepsis

To study the effects of Ac2-26 on AKI in sepsis, we detected kidney histology by HE staining and TEM at 24 h after CLP. The kidney histology is shown in Figure 4. HE staining revealed hemorrhage and edema of tubular epithelial cells, inflammatory cell infiltration and narrowing of kidney tubular lumina in the kidneys of the sepsis group compared with those of the control group (Figure 4A). However, treatment with mimetic peptide Ac2-26 of ANXA1 significantly improved the above kidney histopathological changes in the Ac2-26+sepsis group (Figure 4A). In addition, TEM images showed that the kidney tissue of the sepsis group had significantly swollen

and disorganized microvilli on the surface of renal tubular epithelial cells, nuclear shrinkage, nuclear fragmentation and apoptotic body formation, mitochondrial swelling, partial spinal rupture or disappearance compared to the kidney tissue of mice in the Ac2-26+sepsis group (Figure 4B). Taken together, these results suggest that Ac2-26 improves kidney injury in mice with CLP-induced sepsis.

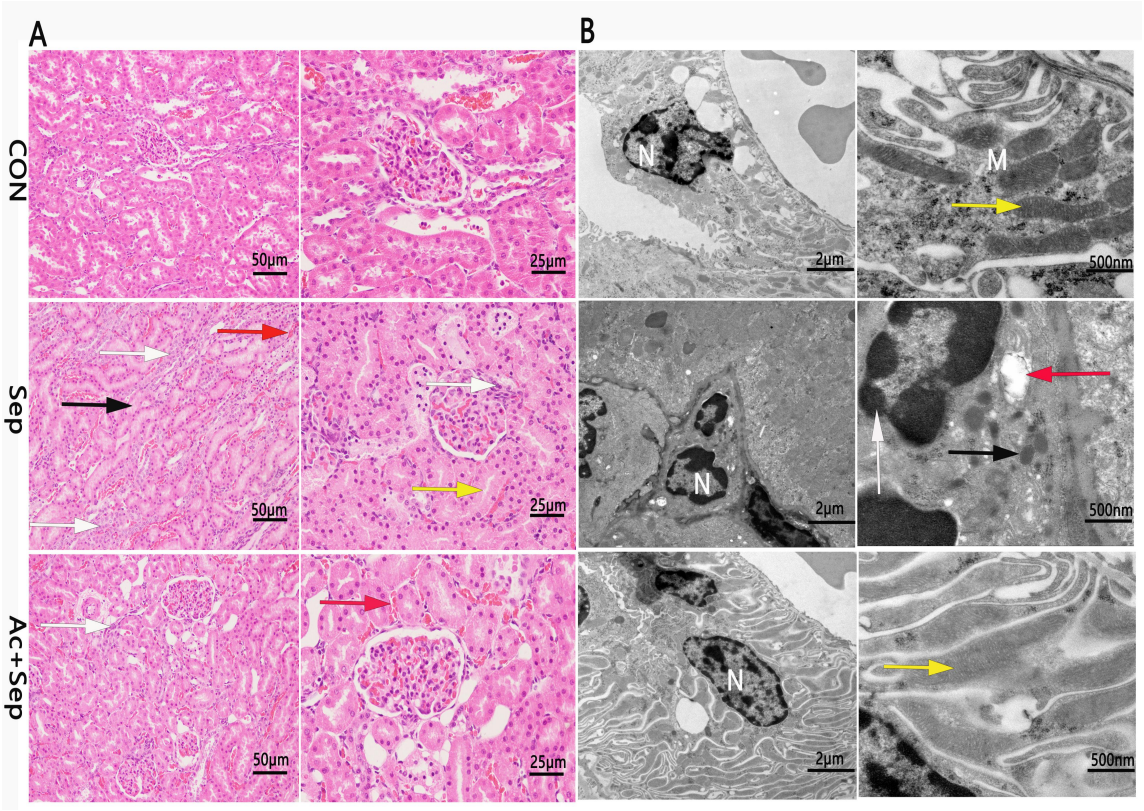

Figure 4. Ac2-26 alleviate pathological damage of kidney tissue of mice with sepsis. (A) and (B) At 24 h after CLP operation, the kidney histopathological changes was detected by HE staining and TEM, respectively. Note: (A): white arrow: inflammatory cells; black arrow: edema; red arrow: hemorrhage; yellow arrow: narrowing of kidney tubular lumina; (×200 or 400). (B): N: nucleus; m: mitochondrion; white arrow: nuclear fragmentation; black arrow: apoptotic body; red arrow: cytoplasmic cavitation; yellow arrow: mitochondrial spinal; (×2900 or 13000). (n = 6 per group).

Ac2-26 inhibited apoptosis in the kidneys of mice with sepsis

To explore whether apoptosis was associated with the protective effects of Ac2-26 on sepsis-induced AKI, the expression of NF-κB, cleaved caspase3, Caspase8 and FADD was detected by ELISA and western blotting. These proteins are considered to be key mediators and markers of apoptosis. Moreover, apoptosis in kidney tissue was measured by TUNEL assay. The protein expression levels of NF-κB, cleaved caspase3, Caspase8 and FADD in kidney tissue of mice in the sepsis group were significantly upregulated compared with those in the control group (Figure 5A). Interestingly, treatment with mimetic peptide Ac2-26 of ANXA1 markedly downregulated the above proteins in the Ac2-26+sepsis group compared to those in the sepsis group (Figure 5A). Furthermore, TUNEL staining results showed that the number of TUNEL-positive cells in the kidney tissue was significantly increased in the sepsis

group compared to that of the control group (Figure 5B). In contrast, in the Ac2-26+sepsis group, treatment with mimetic peptide Ac2-26 of ANXA1 markedly reduced apoptosis compared with that of the sepsis group (Figure 5B). These data suggest that Ac2-26 plays a protective role in sepsis-induced AKI.

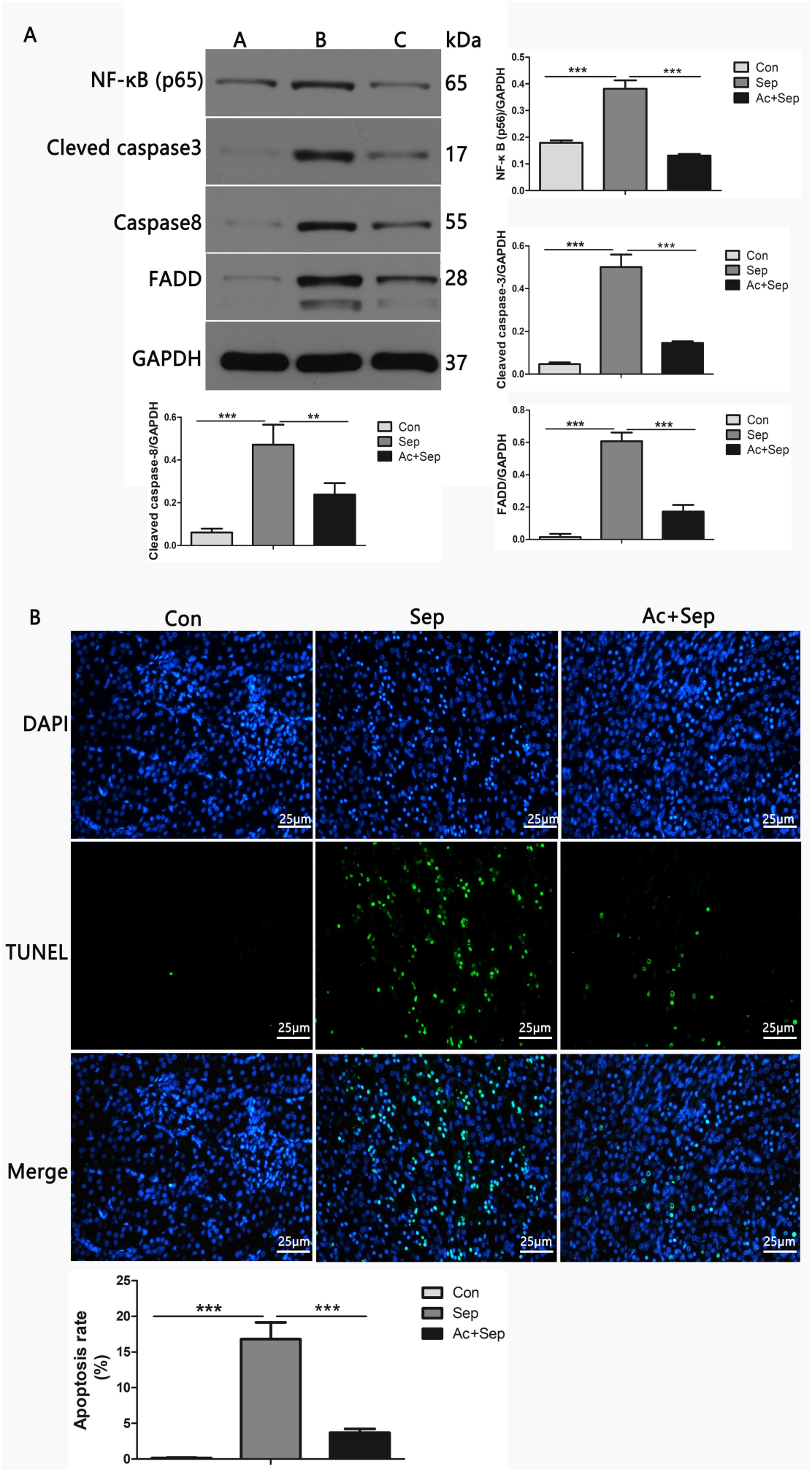
A
A
B
C
kDa
NF-κB (p65)
65
Cleved caspase3
17
Caspase8
55
FADD
28
GAPDH
37
NF-κ B (p56)/GAPDH
Cleaved caspase-3/GAPDH
FADD/GAPDH
Cleaved caspase-8/GAPDH
***
**
Con
Sep
Ac+Sep
B
Con
Sep
Ac+Sep
DAPI
TUNEL
Merge
25μm
Apoptosis rate (%)

Figure 5. Ac2-26 inhibited apoptosis in the kidney of mice with sepsis. (A) A:Con; B:Sep; C:Ac+Sep, at 24 h after CLP operation, the apoptosis-associated molecules of Cleaved caspase3, Caspase8 and FADD in the kidney tissues were detected by western blotting. (B) the apoptosis in kidney tissue was measured by TUNEL assay (×400). Note: (B): TUNEL-positive cells showed green fluorescence; the data are shown as mean ± SD (n = 6 per group, **P*< 0.05, ***P*< 0.01, ****P*<0.001).

Ac2-26 improved the cell viability of HK-2 cells that were stimulated with LPS

The effect of ANXA1 on LPS-induced HK-2 cell injury was determined. The results showed that the viability of cells significantly decreased with increasing LPS concentrations. In contrast, mimetic peptide Ac2-26 of ANXA1 significantly increased the viability of HK-2 cells that were stimulated with LPS. (Figure 6).

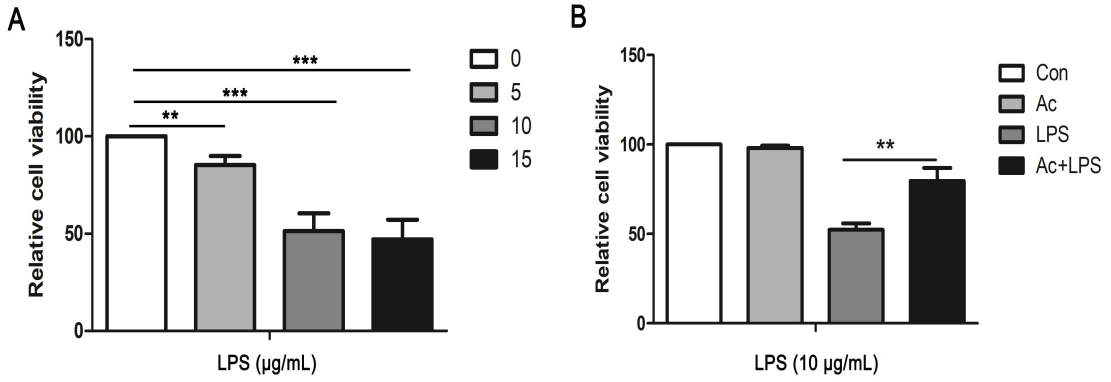

Figure 6. Ac2-26 improved the cell viability of HK-2 cells that were stimulated with LPS. (A) and (B) At 24 h after LPS stimulation, the cell viability of HK-2 cells was detected by CCK-8. Note: the data are shown as mean ± SD (n =6 per group, ***P*< 0.01, ****P*<0.001).

Ac2-26 inhibited the levels of inflammatory cytokines in HK-2 cells that were stimulated with LPS

LPS induced inflammatory damage to HK-2 cells *in vitro*, which is similar to the effects in septic AKI. The expression levels of TNF-α, IL-1β and IL-6 were significantly higher (Figure 7) in the LPS group than in the control group (Figure 7). Interestingly, in the Ac2-26+LPS group, treatment with mimetic peptide Ac2-26 of ANXA1 reduced these cytokines compared with those in the LPS group (Figure 7). These results suggest that Ac2-26 suppresses the production of inflammatory cytokines in HK-2 cells and alleviated LPS-induced HK-2 cell injury.

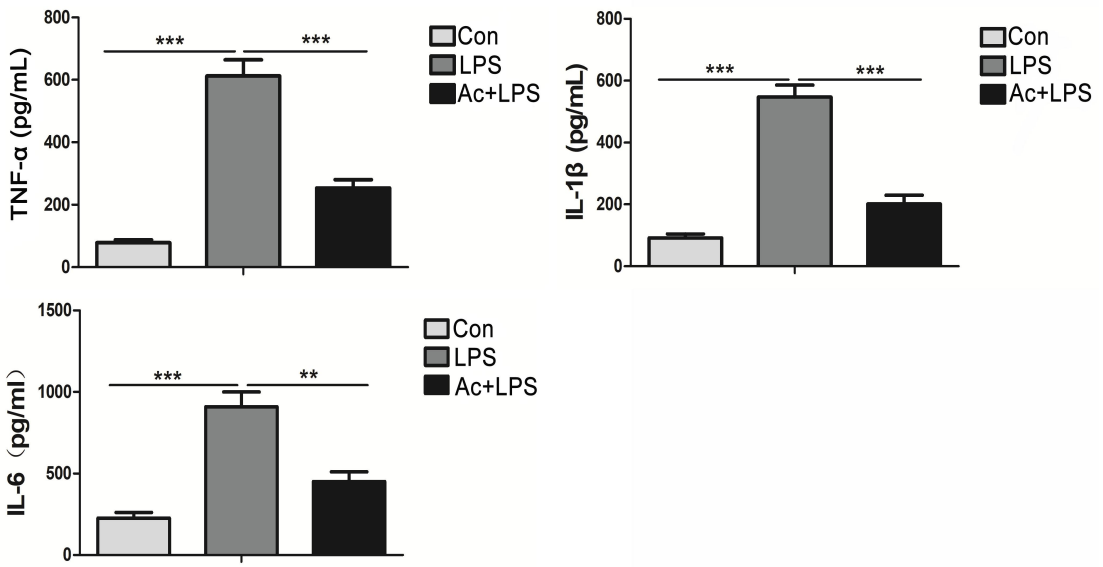

Figure 7. Ac2-26 inhibited the levels of inflammatory cytokines in HK-2 cells that were stimulated with LPS. At 24 h after LPS stimulation, the levels of TNF-α, IL-1β and IL-6 in the HK-2 cells was detected by Elisa. Note: the data are shown as mean ± SD (n = 6 per group, ***P*< 0.01, ****P*<0.001).

Ac2-26 negatively regulated LPS-induced HK-2 cell apoptosis induced by LPS

To further confirm that Ac2-26 regulated LPS-induced HK-2 cell injury, we examined the effect of the ANXA1 mimetic peptide Ac2-26 on LPS-induced apoptosis of HK-cells by western blotting, immunocytochemistry and flow cytometry. Bcl-2 and Bax are important proteins that are involved in regulating apoptosis. The results showed that induction with LPS obviously downregulated the level of Bcl-2 and upregulated the level of Bax in HK-2 cells in the LPS group compared with those in the control group (Figure 8A). However, after treatment with the ANXA1 mimetic peptide Ac2-26, the expression level of Bcl-2 was obviously upregulated, and Bax was downregulated in the HK-2 cells in the Ac2-26+LPS group compared with those in the LPS group (Figure 8A). As well as, after treatment with the ANXA1 mimetic peptide Ac2-26, the expression level of Bcl-2 obviously increased and the expression level of Bax markedly decreased in Ac2-26+LPS group compared with these in LPS group (Figure 8B). Moreover, flow cytometry showed that HK-2 cells in the upper and lower right quadrants are apoptotic cells. The apoptotic rate of HK-2 cells in the LPS group was significantly increased compared to that of the control group (Figure 8C) and was significantly reduced by administration of ANXA1 in the Ac2-26+LPS group compared to that of the sepsis group (Figure 8C).

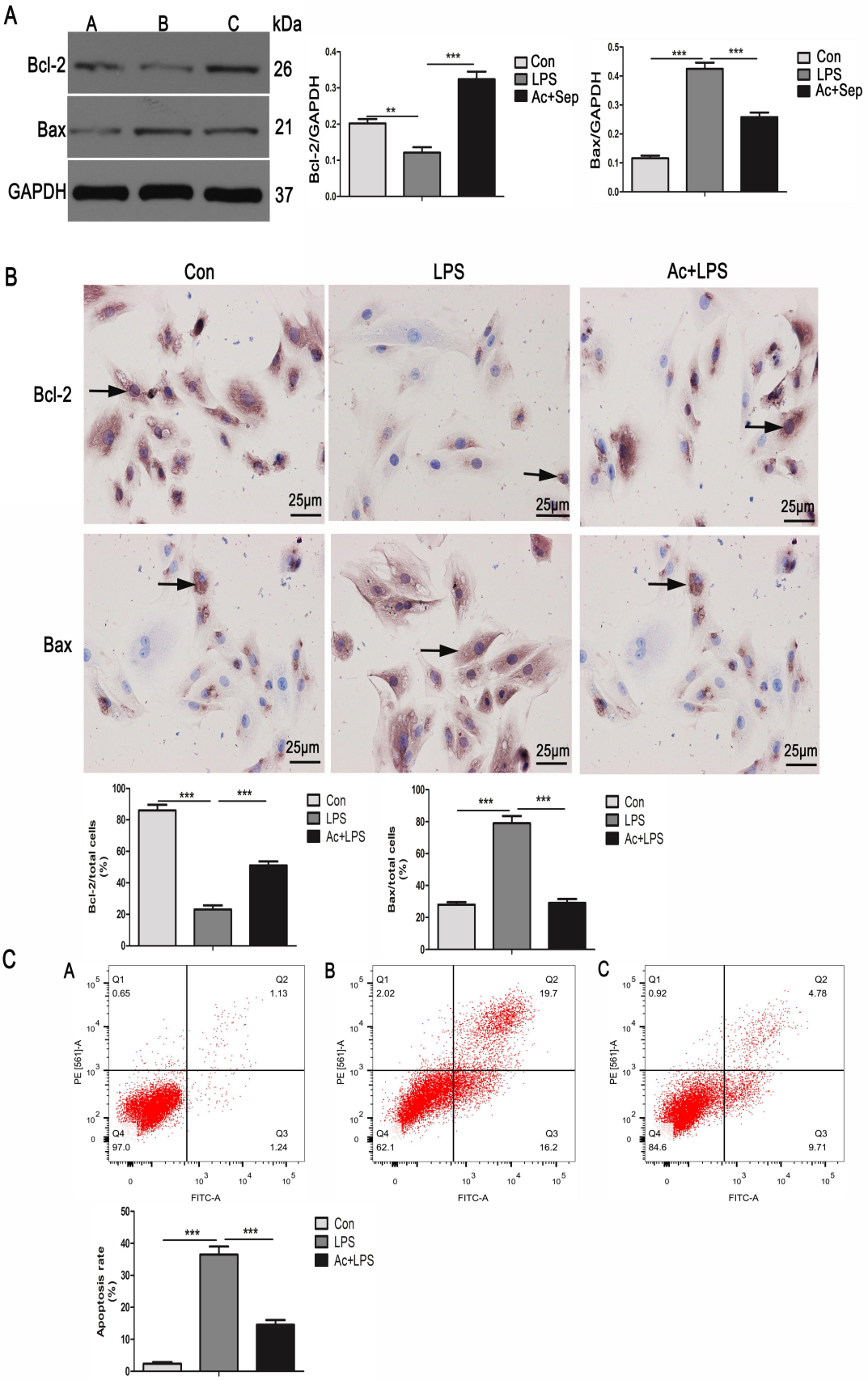

Figure 8. Ac2-26 negatively regulated LPS-induced HK-2 cell apoptosis. (A) and (B) At 24 h after LPS stimulation, the levels of the apoptosis-associated proteins Bcl-2 and Bax in

the HK-2 cells were detected by western blotting and immunocytochemistry (×400). (C) HK-2 cell apoptosis at 24 h after LPS stimulation was detected by flow cytometry. Note: A: Con; B:LPS; C:Ac+LPS group; (B): HK-2 cells stained brownish are immune-positive cells (black arrow); the data are shown as the mean ± SD (n = 6 per group, $^{**}P< 0.01$, $^{***}P<0.001$).

Discussion

Currently, sepsis 3.0 is defined as life-threatening organ dysfunction caused by an uncontrolled inflammatory response [26]. AKI is a common organ dysfunction in patients with sepsis. Hence, the prevention and treatment of the kidney inflammatory response and apoptosis may have clinical value for patients with sepsis. The mimetic peptide Ac2-26 of ANXA1 plays important roles in the control of inflammation and apoptosis [18-19, 22]. ANXA1 is expressed in multiple tissues and organs, such as the heart, lung, brain, and kidney [17]. We recently showed that Ac2-26 protects against myocardial injury in rats with sepsis by negatively regulating myocardial apoptosis [27]. However, it is unclear whether Ac2-26 has an impact on the pathological process of sepsis-induced AKI. In this study, we found that Ac2-26 inhibited the inflammatory response and apoptosis by regulating the PI3K/IKK-β/NF-κB pathway in septic AKI *in vivo* and *in vitro*. Similarly, PI3K/IKK-β/NF-κB signaling pathway has been reported to be closely related to inflammatory response and AKI [28-29]. The inflammatory response is increasingly recognized as the main trigger for sepsis-induced AKI [30]. LPS is a key molecule in the initiation of sepsis [31]. It was reported that the expression of Toll-like receptor (TLR) and myeloid differentiation factor-88 (MyD88) in the murine adrenal gland is upregulated by LPS induction [32]. In addition, LPS binds with the Toll-like receptor 4 (TLR4)-MD2 complex, which activates the MyD88 signaling pathway [33], resulting in phosphorylation downstream of IκBα kinase (IKK) [34]. Phosphorylated IKK stimulates the activation of NF-κB [35], and the activation of NF-κB induces the mass production and release of inflammatory factors [36]. It is currently believed that LXA4 activity is dependent on the N-terminal region of themimetic peptide Ac2-26 of ANXA1 [17, 37]. Studies have shown that LXA4 inhibits the downstream activity of NF-κB by inhibiting the PI3K/Akt signaling pathway, thus playing an anti-inflammatory role [38].

Similarly, in the present study, we found that the expression levels of LXA4 significantly decreased and the levels of MyD88, P-IKKβ, P-PI3K, and NF-κB were upregulated in kidney tissue of mice in the sepsis group compared with those in the control group (Figure 3A) *in vivo*. Additionally, the levels of the inflammatory cytokines TNF-α, IL-1β and IL-6 were significantly higher in the sepsis group and the LPS group than in the control group (Figures 3B and 7) *in vivo* and *in vitro*. Interestingly, we also found that treatment with the mimetic peptide Ac2-26 of ANXA1 significantly increased the level of LXA4, downregulated the expression levels of MyD88, P-IKKβ, P-PI3K, and NF-κB and decreased the levels of TNF-α, IL-1β, and IL-6 in the Ac2-26+sepsis and the Ac2-26+LPS groups compared with those of the sepsis and the LPS groups (Figures 2, 3A, 3B and 7) *in vivo* and *in vitro*. Additionally, HE staining and TEM revealed that treatment with ANXA1 Ac2-26 peptide markedly alleviated pathological injury in kidney tissue in the Ac2-26+sepsis

group compared with that in the sepsis group (Figure 4A and 4B). ANXA1 obviously reversed the above changes, suggesting that ANXA1 plays a protective role in sepsis-associated inflammatory injury *in vivo* and *in vitro*.

Moreover, apoptosis is closely related to acute kidney injury in sepsis [11-13, 39]. NF-κB is an important link in apoptosis regulation [40]. It has been reported that LXA4 inhibits hepatic apoptosis by negatively regulating the activity of NF-κB [41]. In rats with cerebral ischaemia, NF-κB promotes apoptosis by increasing the level of Bax [42]. In addition, previous studies have shown that apoptosis requires activation of the PI3K/Akt/IKK-α/NF-κB pathway in human salivary adenoid cystic carcinoma.[43] In this study, our results demonstrated that the expression levels of the proapoptotic proteins NF-κB, cleaved caspase3, Caspase8, FADD, and Bax were obviously upregulated and that the level of the antiapoptotic protein Bcl-2 was obviously downregulated in the sepsis and the LPS groups compared with those in the control group (Figures 5A, 8A and 8B) *in vivo* and *in vitro*. Moreover, TUNEL staining and flow cytometry revealed that significant renal tissue and cell apoptosis were observed in the sepsis and LPS groups compared with those in the control group (Figures 5B and 8C) *in vivo* and *in vitro*. Conversely, our data demonstrated that treatment with the mimetic peptide Ac2-26 of ANXA1 markedly downregulated the levels of the proapoptotic proteins NF-κB, cleaved caspase3, Caspase8, FADD, and Bax, upregulated the level of the antiapoptotic protein Bcl-2, and inhibited renal tissue and cell apoptosis in the Ac2-26+sepsis and Ac2-26+LPS groups compared with those in the sepsis and LPS groups (Figure 5A, 5B, 8A and 8C). Moreover, the kidney function and survival rate of mice were significantly improved after treatment with the mimetic peptide Ac2-26 of ANXA1 in the Ac2-26+sepsis group compared to those in the sepsis group (Figure 1A and 1B). Taken together, the regulating of the LXA4/PI3K/IKK-β/NF-κB signaling pathway, which attenuated the inflammatory response and apoptosis in kidney tissue and HK-2 cells during sepsis, may contribute to the protective effect of ANXA1 on sepsis-induced AKI.

Conclusions

In summary, the *in vivo* and *in vitro* data of our studies revealed that the LXA4/PI3K/IKK-β/NF-κB pathway was activated during sepsis and contributed to sepsis-induced AKI by enhancing the production and release of proinflammatory factors and proapoptotic proteins in kidney tissue and HK-2 cells, respectively. Administration of the mimetic peptide Ac2-26 of ANXA1 ameliorated septic AKI by inhibiting the inflammatory response and apoptosis by regulating the LXA4/PI3K/IKK-β/NF-κB pathway (Figure 9). These results might help in the development of new therapeutic strategy for treatment sepsis-associated AKI.

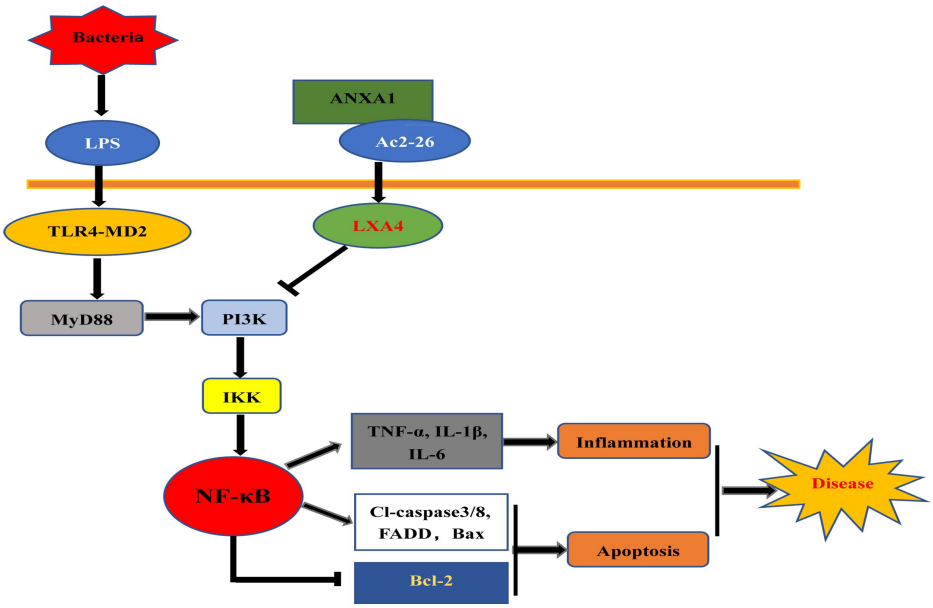

Figure 9. The potential mechanisms of mimetic peptide Ac2-26 of ANXA1 could ameliorate septic AKI by regulating the LXA4/PI3K/IKK-β/NF-κB pathway. The arrow represents promotion, the "tee" head represents inhibition.

Ethics approval and consent to participate

This study was approved by the Ethical Committee of Hubei Cancer Hospital is Affiliated to Tongji Medical College of Huazhong University of Science and Technology.

Consent for publication

Not applicable.

Conflicts of Interest

The authors have declared no conflict of interest.

Funding

This work was financially supported by Joint Fund Project of Health and Family Planning Commission of Hubei Province [grant number WJ2019H130].

Author Contributions

Yanlei Zheng performed the experiments, analyzed the data, prepared the figures, and wrote the manuscript; Ronghua Hu performed the experiments, interpreted the data; Li Zhang provided laboratory space and funding, designed the study, analyzed the data.

Acknowledgements

Not applicable.

Availability of data and material

All data generated or analyzed during this study are included in this published article.

References

1. C. Fleischmann, A. Scherag, N.K. Adhikari, et al. Assessment of global incidence and mortality of hospital-treated sepsis. Current estimates and limitations. Am J Respir Crit Care Med. 2016, 193(3):259-272.

2. Zarjou A , Agarwal A . Sepsis and Acute Kidney Injury. Journal of the American Society of

Nephrology. 2011, 22(6):999-1006.
3. Gao Y , Dai X , Li Y , et al. Role of Parkin-mediated mitophagy in the protective effect of polydatin in sepsis-induced acute kidney injury. Journal of Translational Medicine. 2020, 18:114.
4. Moeckel, Gilbert W . Pathologic Perspectives on Acute Tubular Injury Assessment in the Kidney Biopsy. Seminars in Nephrology. 2018, 38(1):21-30.
5. Chua H R , Wong W K , Ong V H , et al. Extended Mortality and Chronic Kidney Disease After Septic Acute Kidney Injury. Journal of Intensive Care Medicine. 2018, 088506661876461.
6. Bellomo R , Kellum J A , Ronco C , et al. Acute kidney injury in sepsis. Intensive Care Medicine. 2017, 43(6):816-828.
7. Ricci Z , Ronco C. Pathogenesis of Acute Kidney Injury During Sepsis. Current Drug Targets. 2007, 10(12): 1179-1183.
8. Otero R M , Nguyen H B , Huang D T , et al. Early goal-directed therapy in severe sepsis and septic shock revisited - Concepts, controversies, and contemporary findings. Chest. 2016, 130(5):1579-1595.
9. Ergin B,Kapucu A,Demirci-Tansel C.The renal microcirculation in sepsis. Nephrol Dial Transplant. 2015, 30:169-177.
10. Morrell E D , Kellum J A , Núria M Pastor-Soler, et al. Septic acute kidney injury: molecular mechanisms and the importance of stratification and targeting therapy. Critical Care. 2014, 18(5):501.
11. Forschbach V , Goppelt-Struebe M , Kunzelmann K , et al. Anoctamin 6 is localized in the primary cilium of renal tubular cells and is involved in apoptosis-dependent cyst lumen formation. Cell Death and Disease. 2015, 6(10):e1899.
12. Kaushal, Gur P . Autophagy protects proximal tubular cells from injury and apoptosis. Kidney International. 2012, 82(12):1250-1253.
13. Liu J , Abdel-Razek O , Liu Z , et al. Role of Surfactant Proteins A and D in Sepsis-Induced Acute Kidney Injury. Shock. 2015;43(1):31-38.
14. Beutler B , Rietschel E T . Timeline: Innate immune sensing and its roots: the story of endotoxin. Nat Rev Immunol. 2003, 3(2):169-176.
15. Doi K , Leelahavanichkul A , Yuen P S T , et al. Animal models of sepsis and sepsis-induced kidney injury. The Journal of clinical investigation. 2009, 119(10):2868-2878.
16. Sugimoto Michelle Amantéa, Priscila V J , Martins T M , et al. Annexin A1 and the Resolution of Inflammation: Modulation of Neutrophil Recruitment, Apoptosis, and Clearance. Journal of Immunology Research. 2016, 8239258.
17. Perretti M , Dalli J . Exploiting the Annexin A1 pathway for the development of novel anti-inflammatory therapeutics. British Journal of Pharmacology. 2009, 158(4):936-946.
18. Costa, Maurício B, Mimura K K O , Freitas A A , et al. Mast cell heterogeneity and anti-inflammatory annexin A1 expression in leprosy skin lesions. Microbial Pathogenesis. 2018, 118:277-284.
19. Horlacher T , Noti C , De Paz J L , et al. Characterization of Annexin A1 Glycan Binding Reveals Binding to Highly Sulfated Glycans with Preference for Highly Sulfated Heparan Sulfate and Heparin. Biochemistry. 2011, 50(13):2650-2659.
20. Yang Y H , Morand E , Leech M. Annexin A1: potential for glucocorticoid sparing in RA. Nature Reviews Rheumatology. 2013, 9(10):595-603.
21.Wen-I L , Shu-Yu W , Geng-Chin W , et al. Ac2-26, an Annexin A1 Peptide, Attenuates

Ischemia-Reperfusion-Induced Acute Lung Injury. International Journal of Molecular Sciences. 2017, 18(8):1771.
22. Maderna P , Cottell D C , Toivonen T , et al. FPR2/ALX receptor expression and internalization are critical for lipoxin A4 and annexin-derived peptide-stimulated phagocytosis. The FASEB Journal. 2010, 24(11):4240-4249.
23. Yang JX, Li M, Chen XO, et al. Lipoxin A4 ameliorates lipopolysaccharide-induced lung injury through stimulating epithelial proliferation, reducing epithelial cell apoptosis and inhibits epithelial-mesenchymal transition. Respir Res. 2019, 20(1):192.
24. Zhou Y, Lei J, Xie Q, et al. Fibrinogen-like protein 2 controls sepsis catabasis by interacting with resolvin Dp5. Sci Adv. 2019, 5(11):eaax0629.
25. Ruiz, Stéphanie, Vardon-Bounes F , Merlet-Dupuy V , et al. Sepsis modeling in mice: ligation length is a major severity factor in cecal ligation and puncture. Intensive Care Medicine Experimental. 2016, 4(1):22.
26. Singer M, Deutschman CS, Seymour CW, Shankar-Hari M, Annane D, Bauer M, Bellomo R, Bernard GR, Chiche JD, Coopersmith CM, Hotchkiss RS, Levy MM, Marshall JC, et al. The Third International Consensus Definitions for Sepsis and Septic Shock (Sepsis-3). JAMA. 2016, 315:801–810.
27. Zhang, L., Zheng, Y., Hu, R. et al. Annexin A1 Mimetic Peptide AC2-26 Inhibits Sepsis-induced Cardiomyocyte Apoptosis through LXA4/PI3K/AKT Signaling Pathway. CURR MED SCI. 2018, 38:997–1004.
28. Lin, Bao-Qin, Cui, et al. Timosaponin B-II Ameliorates Palmitate-Induced Insulin Resistance and Inflammation via IRS-1/PI3K/Akt and IKK/NF-kappa B Pathways. American Journal of Chinese Medicine. 2016, 44: 1-15.
29. Iva Potočnjak, Robert Domitrović. Carvacrol attenuates acute kidney injury induced by cisplatin through suppression of ERK and PI3K/Akt activation. Food & Chemical Toxicology. 2016, 98:251-261.
30. Heemskerk S , Masereeuw R , Russel F G M , et al. Selective iNOS inhibition for the treatment of sepsis-induced acute kidney injury. Nature Reviews Nephrology. 2009, 5(11):629-640.
31. Ronco C . Lipopolysaccharide (LPS) from the cellular wall of Gram-negative bacteria, also known as endotoxin, is a key molecule in the pathogenesis of sepsis and septic shock. Preface. Blood Purif. 2014, 37:suppl 1:1.
32. Buss N A P S , Gavins F N E , Cover P O , et al. Targeting the annexin 1-formyl peptide receptor 2/ALX pathway affords protection against bacterial LPS-induced pathologic changes in the murine adrenal cortex. The FASEB Journal. 2015, 29(7):2930.
33. Ryu J K , Kim S J , Rah S H , et al. Reconstruction of LPS Transfer Cascade Reveals Structural Determinants within LBP, CD14, and TLR4-MD2 for Efficient LPS Recognition and Transfer. Immunity. 2016, 46(1):38-50.
34. Hacker H , Vabulas R M , Takeuchi O , et al. Immune Cell Activation by Bacterial Cpg-DNA through Myeloid Differentiation Marker 88 and Tumor Necrosis Factor Receptor-Associated Factor (Traf). Journal of Experimental Medicine. 2000, 192(4):595-600.
35. Zandi E , Chen Y , Karin M . Direct phosphorylation of IkappaB by IKKalpha and IKKbeta: discrimination between free and NF-kappaB-bound substrate. Science. 1998, 281(5381):1360-1363.

36. Tang B , Li X , Ren Y , et al. MicroRNA-29a regulates lipopolysaccharide (LPS)-induced inflammatory responses in murine macrophages through the Akt1/ NF-κB pathway. Experimental Cell Research. 2017, 360(2): 74-80.
37. Brancaleone V , Dalli J , Bena S , et al. Evidence for an Anti-Inflammatory Loop Centered on Polymorphonuclear Leukocyte Formyl Peptide Receptor 2/Lipoxin A4 Receptor and Operative in the Inflamed Microvasculature. The Journal of Immunology. 2011, 186(8):4905-4914.
38. Shi Y , Pan H , Zhang H Z , et al. Lipoxin A4 mitigates experimental autoimmune myocarditis by regulating inflammatory response, NF-κB and PI3K/Akt signaling pathway in mice. European Review for Medical & Pharmacological Sciences. 2017, 21(8):1850-1859.
39. Zhu Y , Fu Y , Lin H . Baicalin Inhibits Renal Cell Apoptosis and Protects Against Acute Kidney Injury in Pediatric Sepsis. Medical Science Monitor. 2016, 22:5109-5115.
40. Zhao G , Yu Y M , Kaneki M , et al. Simvastatin Reduces Burn Injury-Induced Splenic Apoptosis via Downregulation of the TNF-α/NF-κB Pathway. Annals of Surgery. 2016, 261(5):1006-1012.
41. Jiang X , Li Z , Jiang S , et al. Lipoxin A4 exerts protective effects against experimental acute liver failure by inhibiting the NF-κB pathway. International Journal of Molecular Medicine. 2016, 37(3):773-780.
42. Shou Y , Li N , Li L , et al. NF-κB-mediated up-regulation of Bcl-XS and Bax contributes to cytochrome c release in cyanide-induced apoptosis. Journal of Neurochemistry. 2002, 81(4):842–852.
43. Zhi-Jun Sun, Gang Chen, Xiang Hu,et al. Activation of PI3K/Akt/IKK-α/NF-κB signaling pathway is required for the apoptosis-evasion in human salivary adenoid cystic carcinoma: its inhibition by quercetin. Apoptosis. 2010, 15(7):850-863.

Figures

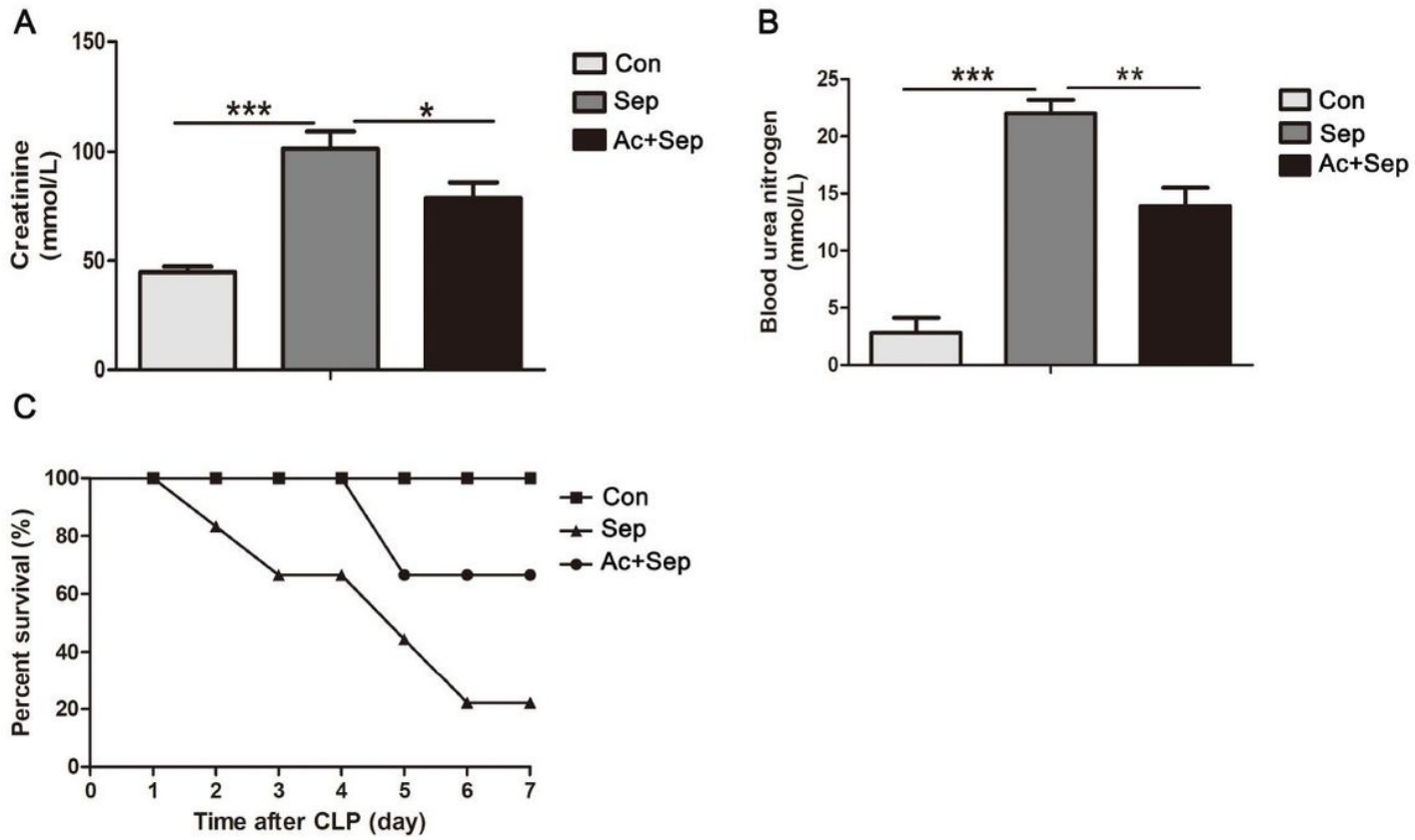

Figure 1

Ac2-26 improved the survival and kidney function of mice with sepsis. (A and B) At 24 h after CLP operation, the levels of Cre and BUN in the kidney tissue were detected by Elisa. (C) the 7 day-survival rate of mice (n= 6 per group). Note: the data are shown as mean ± SD (n = 6 per group, *P < 0.05, **P< 0.01, ***P<0.001).

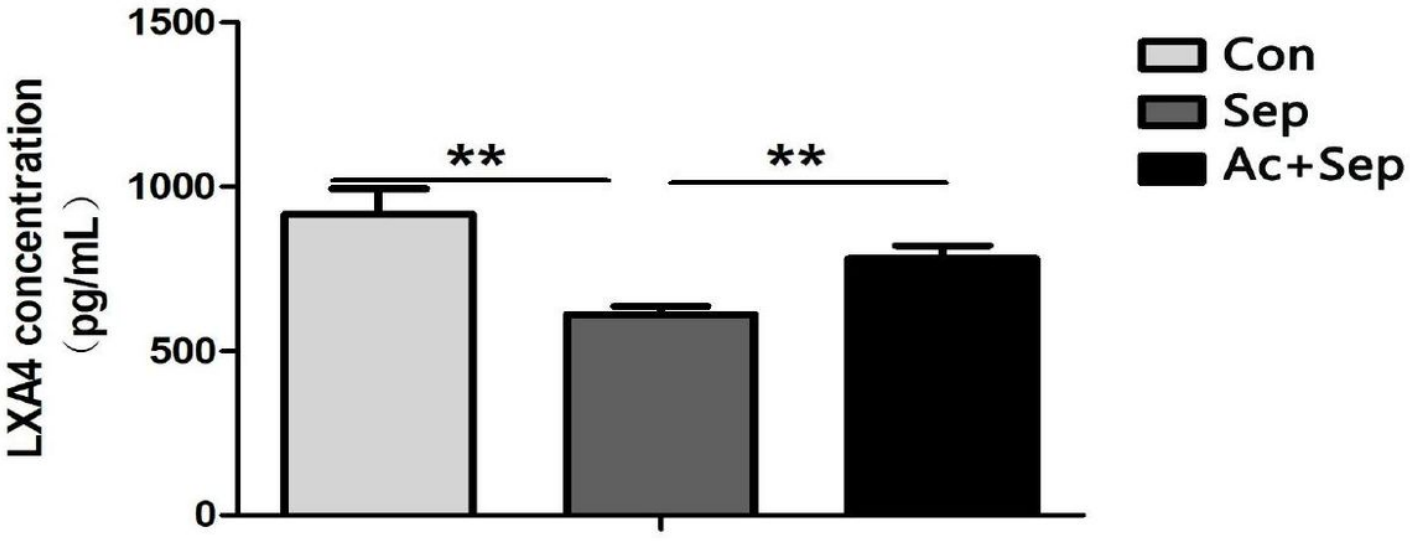

Figure 2

Ac2-26 increased the production of LXA4 in the kidney tissue of mice with sepsis. (A) At 24 h after CLP operation, the LXA4 levels were detected by Elisa. Note: the data are shown as mean ± SD (n = 6 per group, **P< 0.01).

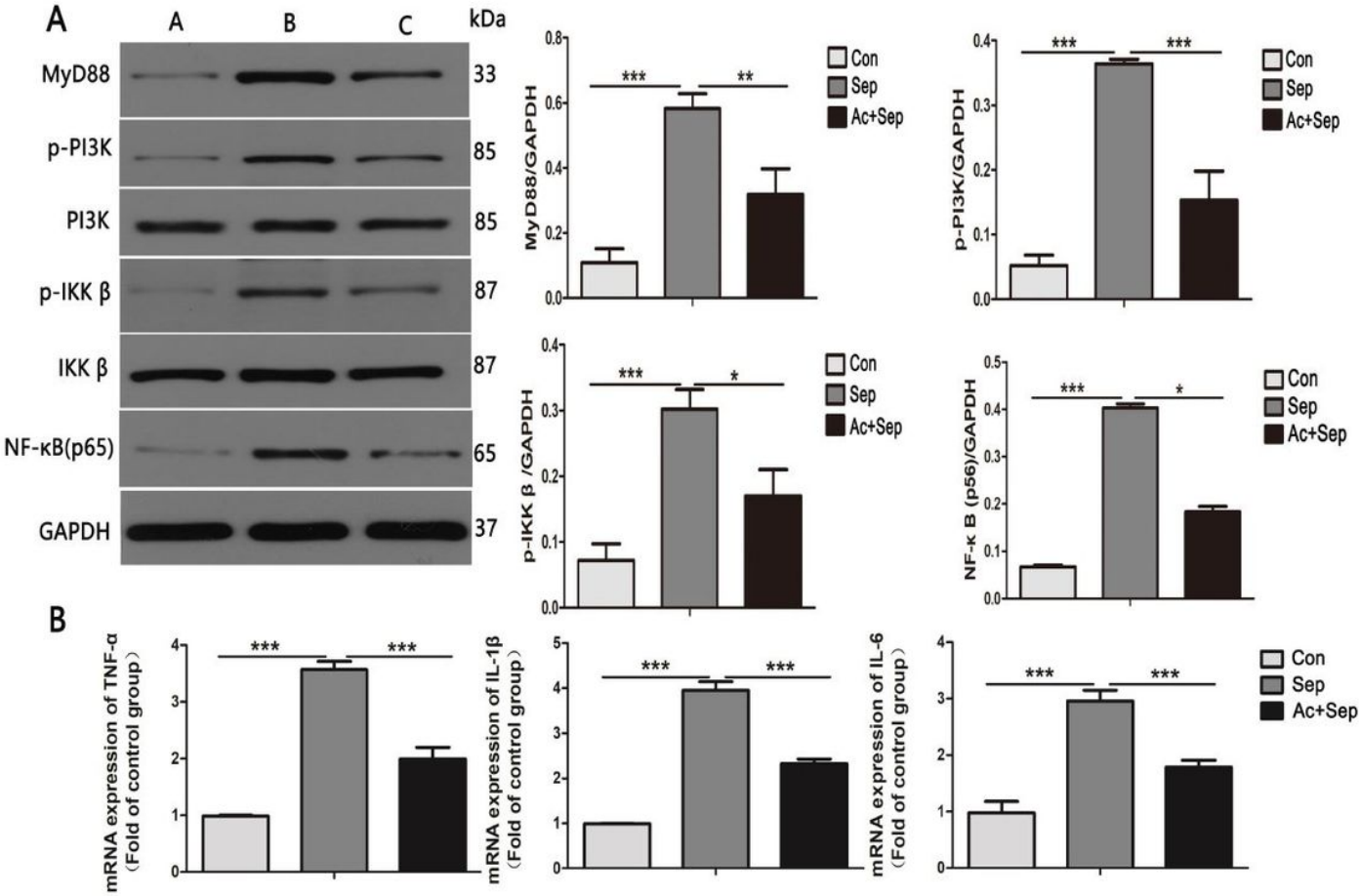

Figure 3

Ac2-26 decreased the production of inflammatory-related cytokines in the kidney tissue of mice with sepsis. (A) At 24 h after CLP operation, the inflammatory cytokines levels were detected by Western blotting, A: Con; B:Sep; C:Ac+Sep; (B) the inflammatory cytokines levels were detected by RT-PCR. Note: the data are shown as mean ± SD (n = 6 per group, *P<0.05, **P< 0.01, ***P<0.001).

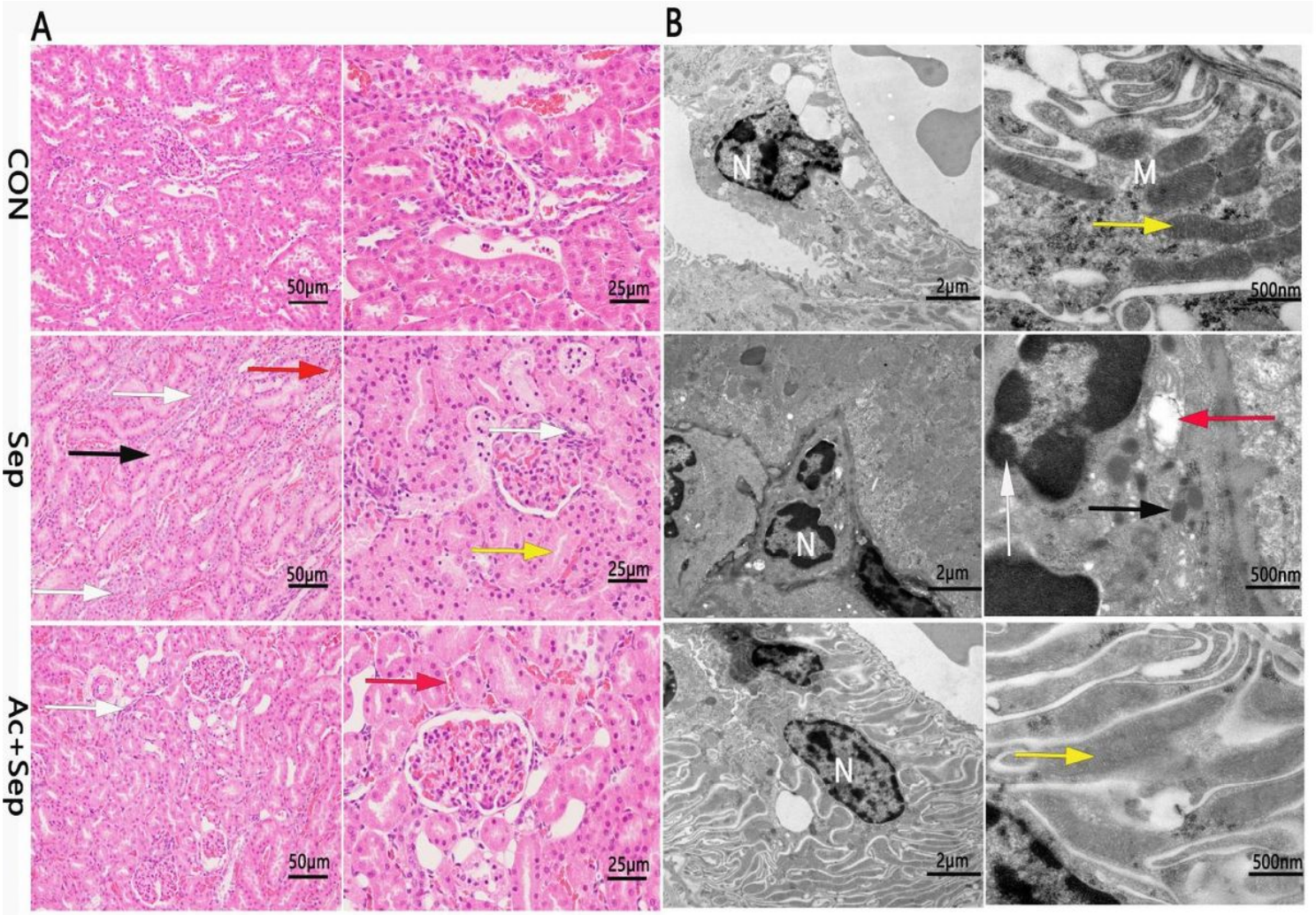

Figure 4

Ac2-26 alleviate pathological damage of kidney tissue of mice with sepsis. (A) and (B) At 24 h after CLP operation, the kidney histopathological changes was detected by HE staining and TEM, respectively. Note: (A): white arrow: inflammatory cells; black arrow: edema; red arrow: hemorrhage; yellow arrow: narrowing of kidney tubular lumina; (×200 or 400). (B): N: nucleus; m: mitochondrion; white arrow: nuclear fragmentation; black arrow: apoptotic body; red arrow: cytoplasmic cavitation; yellow arrow: mitochondrial spinal; (×2900 or 13000). (n = 6 per group).

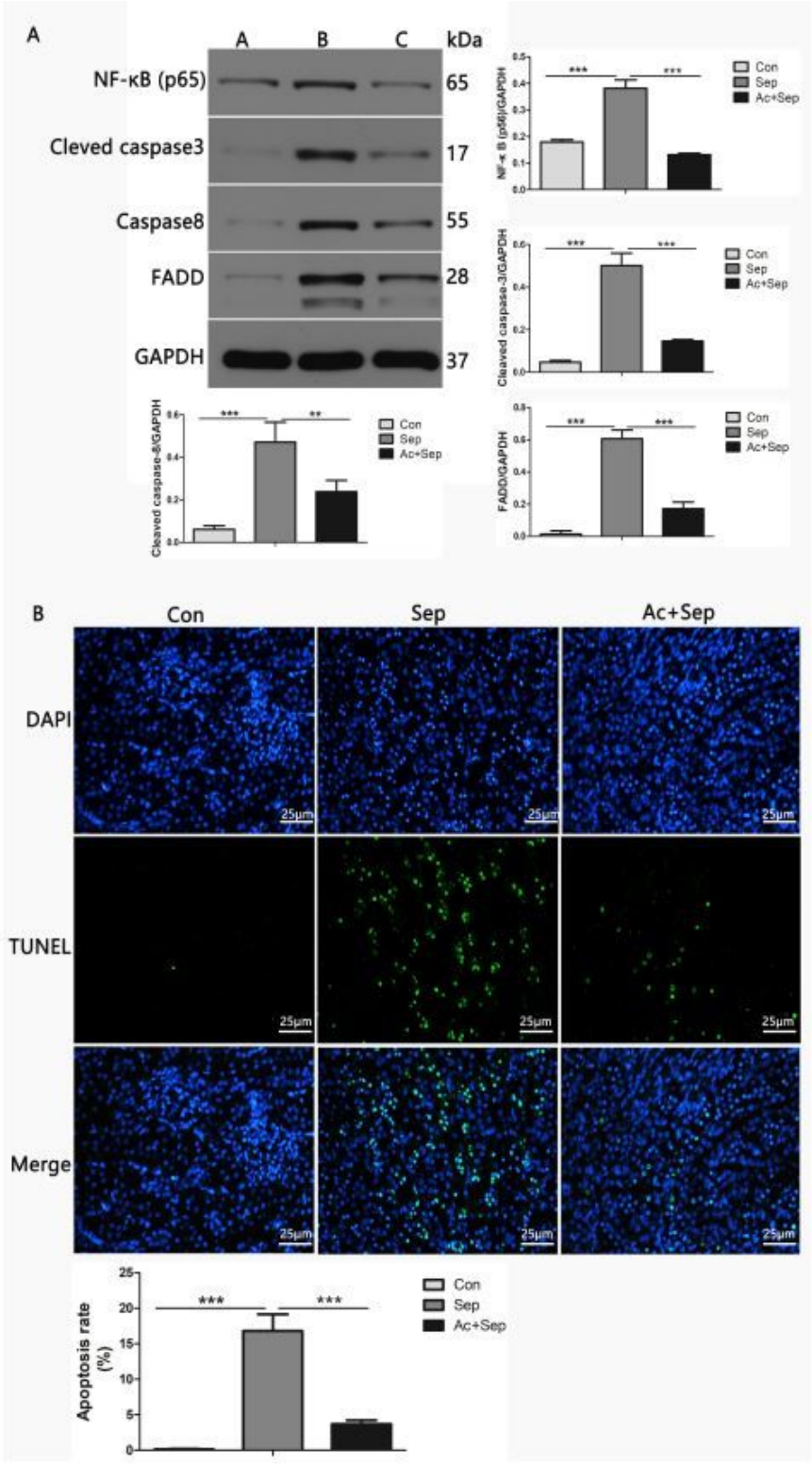

Figure 5

Ac2-26 inhibited apoptosis in the kidney of mice with sepsis. (A) A:Con; B:Sep; C:Ac+Sep, at 24 h after CLP operation, the apoptosis-associated molecules of Cleaved caspase3, Caspase8 and FADD in the kidney tissues were detected by western blotting. (B) the apoptosis in kidney tissue was measured by TUNEL assay (×400). Note: (B): TUNEL-positive cells showed green fluorescence; the data are shown as mean ± SD (n = 6 per group, *P< 0.05, **P< 0.01, ***P<0.001).

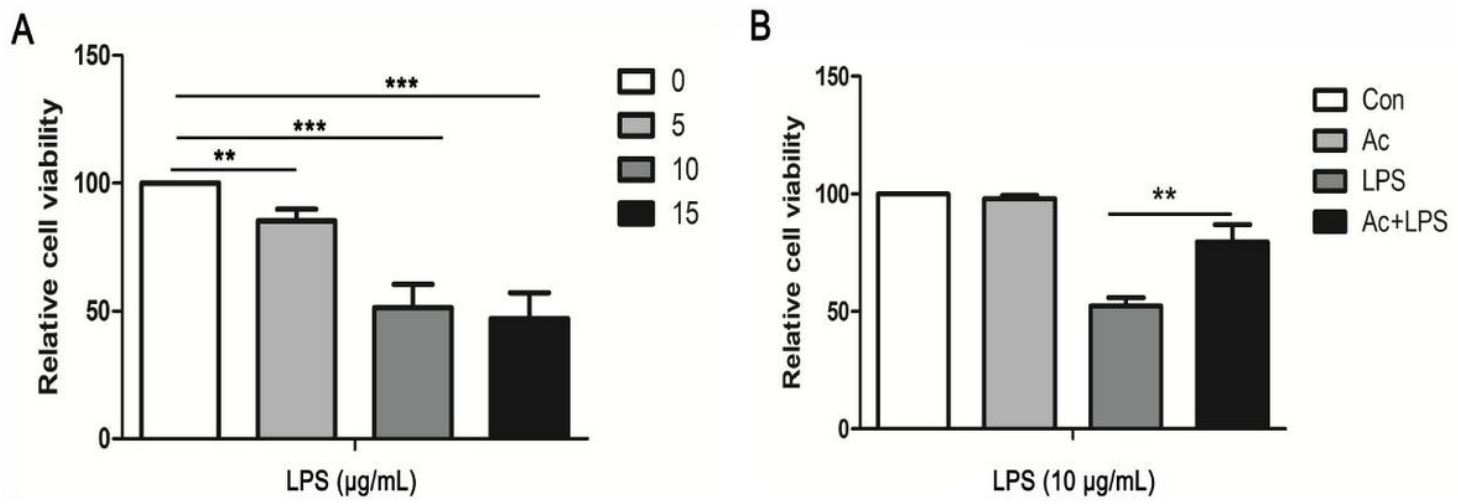

Figure 6

Ac2-26 improved the cell viability of HK-2 cells that were stimulated with LPS. (A) and (B) At 24 h after LPS stimulation, the cell viability of HK-2 cells was detected by CCK-8. Note: the data are shown as mean ± SD (n =6 per group, **P< 0.01, ***P<0.001).

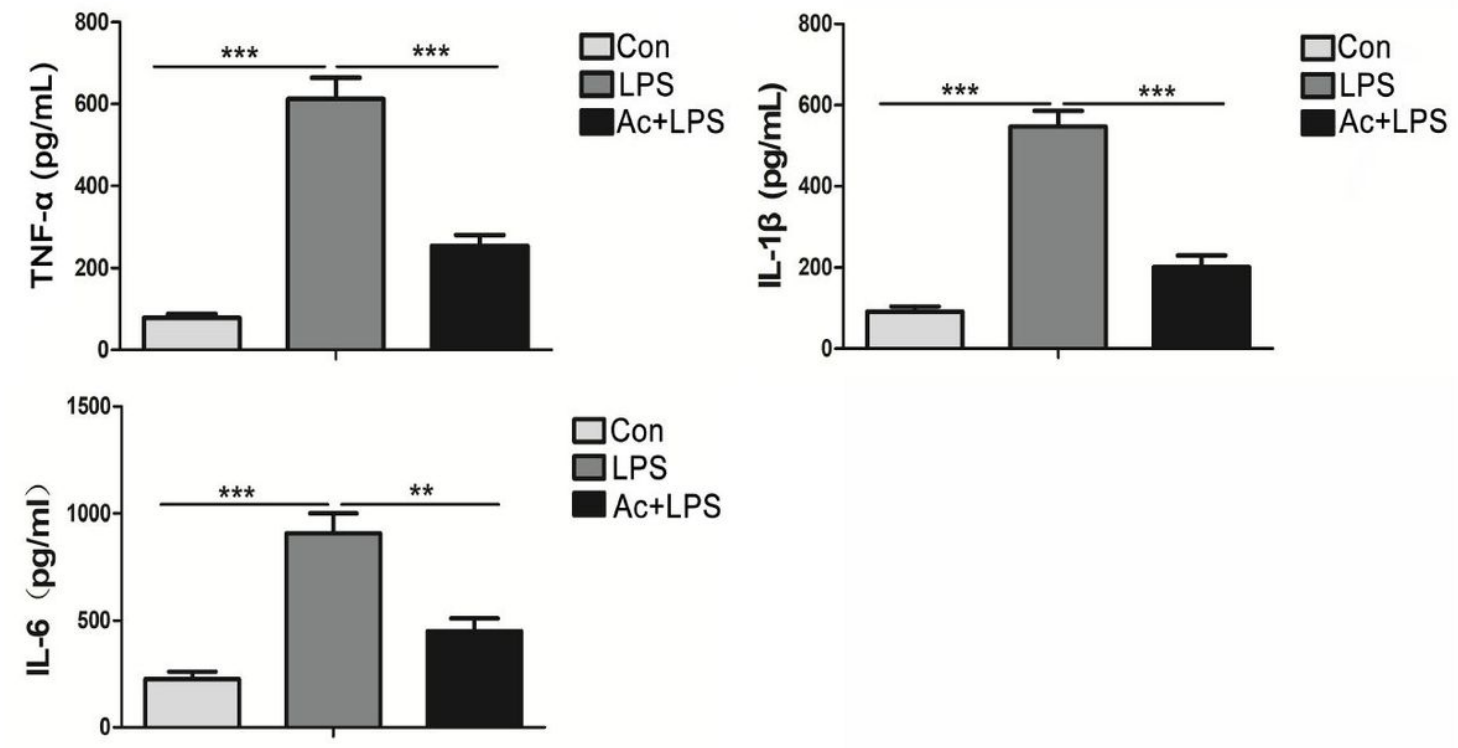

Figure 7

Ac2-26 inhibited the levels of inflammatory cytokines in HK-2 cells that were stimulated with LPS. At 24 h after LPS stimulation, the levels of TNF-α, IL-1β and IL-6 in the HK-2 cells was detected by Elisa. Note: the data are shown as mean ± SD (n = 6 per group, **P< 0.01, ***P<0.001).

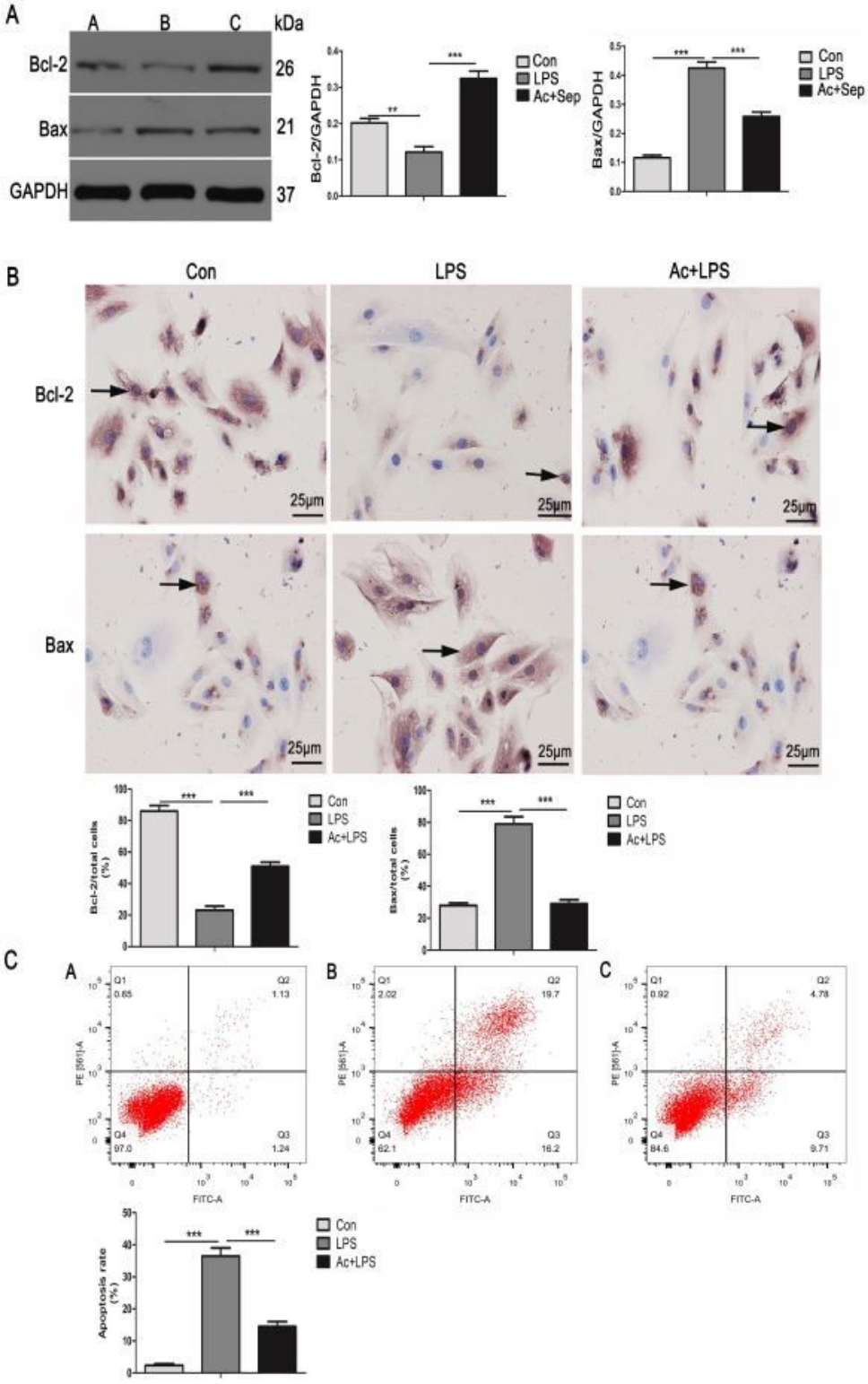

Figure 8

Ac2-26 negatively regulated LPS-induced HK-2 cell apoptosis. (A) and (B) At 24 h after LPS stimulation, the levels of the apoptosis-associated proteins Bcl-2 and Bax in the HK-2 cells were detected by western blotting and immunocytochemistry (×400). (C) HK-2 cell apoptosis at 24 h after LPS stimulation was detected by flow cytometry. Note: A: Con; B:LPS; C:Ac+LPS group; (B): HK-2 cells stained brownish are

immune-positive cells (black arrow); the data are shown as the mean ± SD (n = 6 per group, **P< 0.01, ***P<0.001).

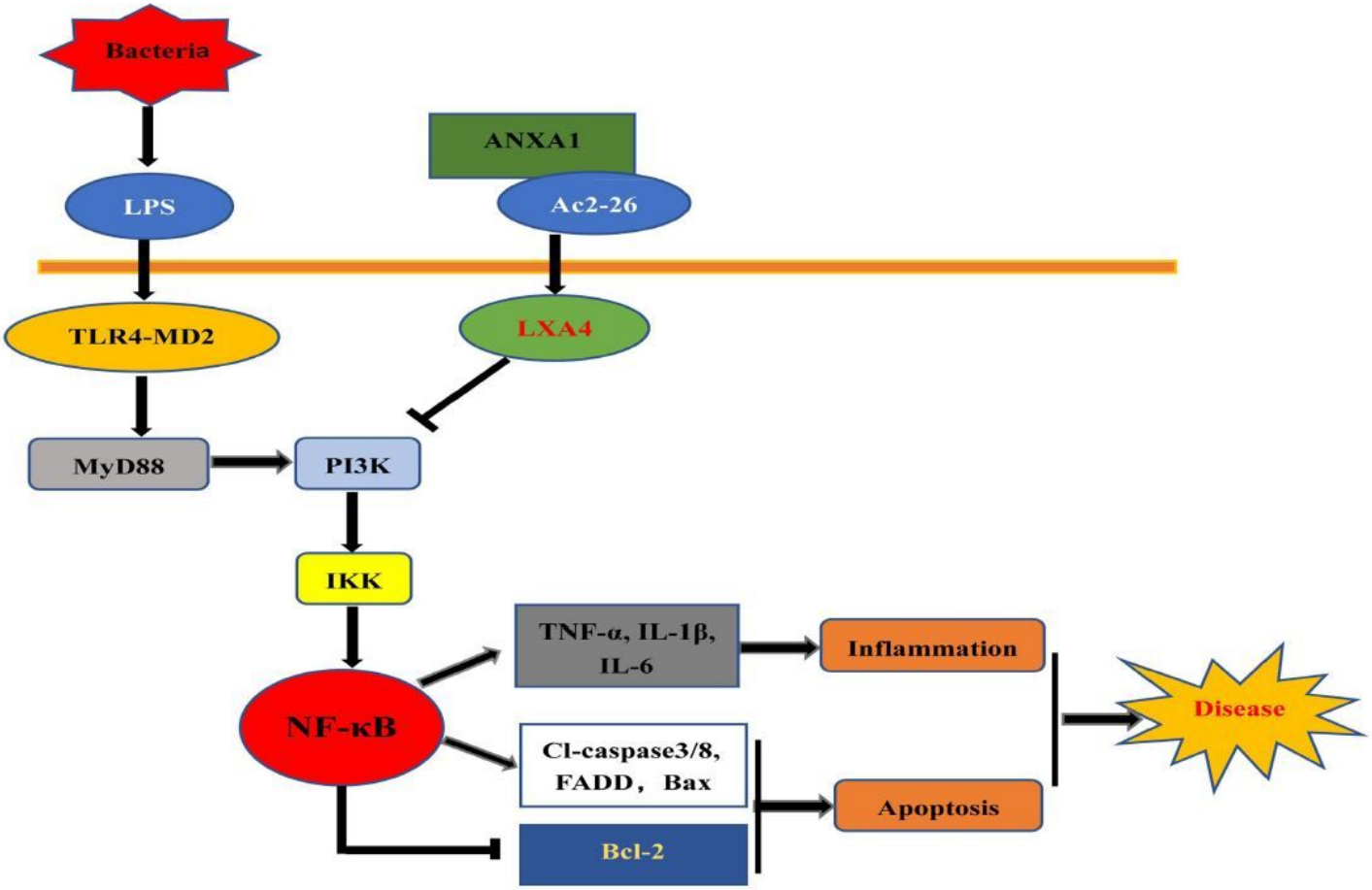

Figure 9

The potential mechanisms of mimetic peptide Ac2-26 of ANXA1 could ameliorate septic AKI by regulating the LXA4/PI3K/IKK-β/NF-κB pathway. The arrow represents promotion, the “tee” head represents inhibition.